STAR-RIS Enabled Downlink Secure NOMA Network Under Imperfect CSI of Eavesdroppers

Hanbo Jia, *Graduate Student Member, IEEE*, Lin Ma, *Senior Member, IEEE*, and Shahrokh Valaee, *Fellow, IEEE*

***Abstract*— Reconfigurable intelligence surface (RIS) is regarded as one of the key technologies for the future wireless communications. Recently, simultaneous transmission and reflection (STAR) RIS is proposed to overcome the geographical constraint of the conventional reflection only RIS. In this letter, we model the STAR-RIS enabled downlink secure non-orthogonal multiple access systems under imperfect channel state information (CSI) of eavesdroppers. Specifically, we propose the block coordinate descent based optimization framework to maximize the worst secrecy rate with active beamforming of downlink NOMA at the base station and STAR-RIS coefficients, where the uncertainty of eavesdropper's CSI is transformed by *S-Procedure*. The successive convex approximation and a penalty-based method are utilized to address the non-convexity of the problem. Finally, simulation results demonstrate that the worst secrecy rate of the proposed algorithm outperforms that of the conventional RIS and the other benchmark schemes.**

***Index Terms*— Reconfigurable intelligent surface, simultaneous transmission and reflection, non-orthogonal multiple access, secure communication.**

I. Introduction

WITH the development of metasurfaces, reconfigurable intelligence surface (RIS) is able to provide more degrees of freedom (DoFs) with the ability to modify the wireless channel by intelligent signal reflection [1]. However, the base station (BS) and the user equipment (UE) must be located at the same side of the conventional RIS, which limits its application for more complicated scenarios. Recently, simultaneous transmission and reflection (STAR) RIS with a 360° coverage is proposed to combat the above shortcoming of the conventional RIS under three practical protocols, namely, energy splitting (ES), mode switching (MS), and time switching (TS) [2]. Further, non-orthogonal multiple access (NOMA) is expected to satisfy the spectrum efficiency (SE) requirement of the sixth-generation (6G) wireless networks [3]. Several aspects of a STAR-RIS integrated NOMA network has been studied in the literature, such as the sum coverage range maximization [4] and the power consumption minimization [5], [6].

Manuscript received 25 November 2022; accepted 22 December 2022. Date of publication 3 January 2023; date of current version 10 March 2023. This research was funded by National Key R&D Program of China (2022YFC3801100), National Natural Science Foundation of China (61971162 and 41861134010) and the National Aeronautical Foundation of China (2020Z066015002). The associate editor coordinating the review of this letter and approving it for publication was P. Nguyen. *(Corresponding author: Lin Ma.)*

Hanbo Jia and Lin Ma are with the School of Electronics and Information Engineering, Harbin Institute of Technology, Harbin, Heilongjiang, 150006, China (e-mail: hanbo_jia@stu.hit.edu.cn; malin@hit.edu.cn).

Shahrokh Valaee is with the Department of Electrical and Computer Engineering, University of Toronto, Toronto, ON M5S 3G4, Canada (e-mail: valaee@ece.utoronto.ca).

Digital Object Identifier 10.1109/LCOMM.2023.3233980

In particular, the physical layer security (PLS) of the STAR-RIS assisted network is investigated in several letters. As illustrated in [7], the secrecy rate maximization problem is investigated in multiple-input single-output (MISO) networks under various STAR-RIS protocols, where the BS beamforming vector and the STAR-RIS coefficients are considered. In [8], similar optimization variables are included with the aid of artificial noise, where NOMA is the adopted multiple access technique. However, almost all the letters assume that the channel state information (CSI) of the eavesdropper is perfectly known, which is unrealistic for practical wireless communication systems. The security of uplink NOMA network has been investigated in [9].Reference [10] studies the conventional RIS enhanced convert communication in NOMA systems. The imperfect CSI is also modeled in [11] without considering NOMA systems. In summary, STAR-RIS enabled downlink secure NOMA networks under imperfect CSI remains an open problem.

Motivated by the above observations, in this letter, the PLS of a STAR-RIS enabled downlink MISO NOMA network is studied for the case of imperfect CSI of eavesdroppers. To the best of our knowledge, the proposed model has not yet been investigated. The main contributions of the letter are summarized as follows:

1) We model the worst secrecy rate maximum problem with the aid of STAR-RIS and active beamforming at the BS under imperfect CSI of eavesdroppers to develop a downlink secure MISO NOMA network. This optimization problem is difficult due to the non-convex object function, the coupling of various variables, and the CSI uncertainty.
2) We propose a block coordinate descent (BCD) based optimization algorithm. Specifically, *S-Procedure* is utilized to transform the imperfect CSI to a more traceable form, and the non-convexity and rank-one constraints are handled by the successive convex approximation (SCA) technique and a penalty-based method, respectively. Simulation results demonstrate the superiority of the proposed algorithm compared with the conventional RIS, the fixed ES scheme, and the TS-OMA scheme.

The rest of this letter is organized as follows. Section II provides the system model. Section III introduces the problem formulation. The BCD based optimization under imperfect CSI is presented in Section IV. Section V gives the implementation and performance analysis. Finally, Section VI concludes this letter.

II. System Model

In this letter, the PLS of STAR-RIS enabled downlink MISO NOMA network is studied. Specifically, as illustrated

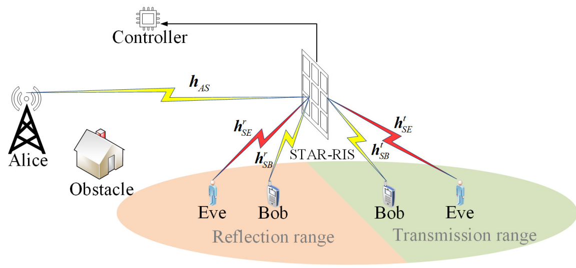

Fig. 1. STAR-RIS enabled downlink secure NOMA network.

in Fig. 1, the direct link between the base station (Alice) and the legitimate UE (Bob) / illegal eavesdropper (Eve) is severely blocked due to an obstacle, where the STAR-RIS is utilized to enhance the PLS by passive beamforming. We aim to maximize the worst secrecy rate with active beamforming on Alice and passive beamforming of STAR-RIS under imperfect CSI of Eves. Assume that Alice is equipped with K antennas. Bobs and Eves are all equipped with a single antenna, and STAR-RIS has M elements. The transmission and reflection coefficients of STAR-RIS are $\boldsymbol{\Phi}_l = \mathrm{diag}\left\{\sqrt{a_1^l}e^{j\phi_1^l}, \sqrt{a_2^l}e^{j\phi_2^l}, \ldots, \sqrt{a_M^l}e^{j\phi_M^l}\right\}, l \in \mathcal{L} \triangleq \{t, r\}$. More practical model of STAR-RIS will be studied in our future work [12]. We assume that the STAR-RIS works on the ES protocol due to the higher flexibility compared with the MS protocol and the TS protocol [2]. Hence, the power constraint must be satisfied such that $a_m^t + a_m^r = 1, \forall m \in \mathcal{M} \triangleq \{1, 2, \ldots, M\}$.

The coverage of STAR-RIS is divided into the transmission range and the reflection range. We assume that a transmission Bob and a reflection Bob are paired in the same resource block in the presence of two illegal Eves [13]. Non-colluding wiretapping is considered in this letter where Eves only eavesdrop the confidential information of the same range. All the channels are modeled as the Rician fading channel, such as the channel between Alice and STAR-RIS, $\boldsymbol{h}_{AS} \in \mathbb{C}^{M\times K}$, can be expressed as

$$\boldsymbol{h}_{AS} = \sqrt{\frac{\rho_0}{(d_{AS})^{\alpha}}}\left(\sqrt{\frac{\beta}{1+\beta}}\bar{\boldsymbol{h}}_{AS} + \sqrt{\frac{1}{1+\beta}}\tilde{\boldsymbol{h}}_{AS}\right), \quad (1)$$

where d_{AS} is the distance between Alice and STAR-RIS, ρ_0 is the path loss at the reference distance, α is the path loss exponent, β is the Rician factor, $\bar{\boldsymbol{h}}_{AS} \in \mathbb{C}^{M\times K}$ is the line-of-sight (LoS) component related to the steering vector function, and $\tilde{\boldsymbol{h}}_{AS} \in \mathbb{C}^{M\times K}$ is the non-LoS (NLoS) component, which can be modeled as a circularly symmetric complex Gaussian (CSCG) random variable with zero mean and unit variance. The channel between STAR-RIS and l Bob $\boldsymbol{h}_{SB}^l \in \mathbb{C}^{M\times 1}$, and STAR-RIS and l Eve $\boldsymbol{h}_{SE}^l \in \mathbb{C}^{M\times 1}$ are similar to $\boldsymbol{h}_{AS}$, therefore are omitted for simplicity. Among various channel estimation algorithms such as anchor-assisted channel estimation proposed recently [14], we assume the CSI between Alice and STAR-RIS, STAR-RIS and Bobs are perfectly known [15]. Moreover, the signal leakage from Eves can be utilized for the coarse channel estimation at Alice [15]. Therefore, a deterministic model is utilized to describe the imperfect CSI of Eves, which consists of a CSI estimation $\bar{\boldsymbol{h}}_{SE}^l$ and an estimation error $\Delta\boldsymbol{h}_{SE}^l$ with norms bounded by ϵ_l [15]. Therefore, $\boldsymbol{h}_{SE}^l \in \mathbb{C}^{M\times 1}$ can be expressed as

$$\boldsymbol{h}_{SE}^l = \bar{\boldsymbol{h}}_{SE}^l + \Delta\boldsymbol{h}_{SE}^l, \quad (2)$$

$$\Omega^l \triangleq \left\{\Delta\boldsymbol{h}_{SE}^l \in \mathbb{C}^{M\times 1} : \left\|\Delta\boldsymbol{h}_{SE}^l\right\| \le \epsilon_l\right\}. \quad (3)$$

Considering the NOMA scheme, the transmitted signal at Alice is $S = \sum_l \boldsymbol{\omega}_l s_l$, where $\boldsymbol{\omega}_l \in \mathbb{C}^{K\times 1}$ is the active beamforming vector of the l symbol s_l. In this letter, we assume that the imperfect successive interference cancellation (SIC) is carried out by Bobs, and Eves have the ability to eliminate the interference perfectly. In addition, Eves only wiretap the Bob in the same range without any collusion. Hence, for $\forall l, l' \in \mathcal{L}$, the SINR of l Bob decoding l' message and l Eve decoding l message can be expressed as

$$\mathrm{SINR}_B^{l'\to l} = \frac{\left|(\boldsymbol{h}_{SB}^l)^H\boldsymbol{\Phi}_l\boldsymbol{h}_{AS}\boldsymbol{\omega}_{l'}\right|^2}{\sum_{\Omega(i)>\Omega(l')}\left|(\boldsymbol{h}_{SB}^l)^H\boldsymbol{\Phi}_l\boldsymbol{h}_{AS}\boldsymbol{\omega}_i\right|^2 + I_B^{l'\to l} + \sigma^2}, \quad (4)$$

$$\mathrm{SINR}_E^{l\to l} = \frac{\left|(\boldsymbol{h}_{SE}^l)^H\boldsymbol{\Phi}_l\boldsymbol{h}_{AS}\boldsymbol{\omega}_l\right|^2}{\sigma^2}, \quad (5)$$

where $\Omega(l)$ denotes the decoding order of l Bob, $I_B^{l'\to l} = \eta\sum_{\Omega(j)<\Omega(l')}\left|(\boldsymbol{h}_{SB}^l)^H\boldsymbol{\Phi}_l\boldsymbol{h}_{AS}\boldsymbol{\omega}_j\right|^2$ is the residual interference introduced by imperfect SIC, and $\eta \in [0, 1]$ represents the efficiency of SIC. The achievable rates of Bobs and Eves are $R_B^{l'\to l} = \log_2(1+\mathrm{SINR}_B^{l'\to l})$ and $R_E^{l\to l} = \log_2(1+\mathrm{SINR}_E^{l\to l})$. Moreover, to guarantee that SIC can be performed successfully, the constraint that $R_B^{k\to l} \ge R_B^{k\to k}$ for $\Omega(k) < \Omega(l)$ must be satisfied.

According to the above derivation, the maximum achievable rate of Eves is $\max_{\Delta\boldsymbol{h}_{SE}^l\in\Omega^l} R_E^{l\to l}$. Therefore, the worst secrecy rate related to the uncertainty of Eves CSI can be expressed as

$$R_S = \sum_l\left[R_B^{l\to l} - \max_{\Delta\boldsymbol{h}_{SE}^l\in\Omega^l} R_E^{l\to l}\right]^+, \quad (6)$$

where $[x]^+ = \max\{x, 0\}$. From the definition of (6), Eves cannot wiretap the message in a different range. Nevertheless, relevant research of the colluding Eves will be carried out in our future research.

III. Problem Formulation

In order to maximize the worst secrecy rate, the beamforming vector for different users, and the transmission and reflection coefficients of STAR-RIS are required to be jointly optimized. Therefore, the following optimization problem is proposed

$$\max_{\boldsymbol{\omega}_l, \boldsymbol{\Phi}_l, \ \forall l} R_S \quad (7a)$$

$$\text{s.t.} \ \sum_l \|\boldsymbol{\omega}_l\| \le P_{\max}, \quad \forall l, \quad (7b)$$

$$R_B^{l\to l} \ge C_B, \forall l, \quad (7c)$$

$$\max_{\Delta\boldsymbol{h}_{SE}^l\in\Omega^l} R_E^{l\to l} \le C_E, \quad \forall l, \quad (7d)$$

$$0 \le \phi_m^l \le 2\pi, \quad \forall l, m, \quad (7e)$$

$$a_m^l + a_m^{l'} = 1, \quad \forall l, m, l' \neq l, \tag{7f}$$
$$R_B^{k\to l} \geq R_B^{k\to k}, \quad \Omega(k) < \Omega(l), \tag{7g}$$

where (7b) is related to the maximum transmission power constraint of Alice, (7c) is to satisfy the quality of service (QoS) requirements of Bobs with the threshold C_B, (7d) is to ensure the achievable rate of Eves below the threshold C_E, (7e) is due to the phase shift of STAR-RIS, (7f) is the power constraint of the ES protocol, and (7g) is related to decoding, which ensures a successful SIC. Actually, the decoding order $\Omega(l)$ of NOMA can also be modified to enhance the PLS by the propagation channel reconstruction ability of STAR-RIS. Hence, we solve (7) for all available $\Omega(l)$ (two cases for 2 users) to find the maximum secrecy rate R_S. Next, we introduce the slack variable $\tau^{l\to l}$ to transform (7) to a more tractable form

$$\max_{\boldsymbol{\omega}_l, \boldsymbol{\Phi}_l, \tau^{l\to l}, P^{l\to l}, \forall l} \sum_l \left[R_B^{l\to l} - \log_2(1+\tau^{l\to l})\right]^+ \tag{8a}$$
$$\text{s.t. } \tau^{l\to l} \geq \max_{\Delta \boldsymbol{h}_{SE}^l \in \Omega^l} \mathrm{SINR}_E^{l\to l}, \quad \forall l, \tag{8b}$$
$$\tau^{l\to l} \leq 2^{C_E} - 1, \quad \forall l, \tag{8c}$$
$$(7\text{b}) - (7\text{c}), (7\text{e}) - (7\text{g}).$$

Using the *Generalized S-Procedure* in [16], the uncertain CSI of the wiretap channel related constraint, (8b), is transformed to the equivalent form

$$\begin{bmatrix} \tau^{l\to l}\sigma^2 - P^{l\to l} + \tilde{\boldsymbol{Q}}^{l\to l} & (\bar{\boldsymbol{h}}_{SE}^l)^H \boldsymbol{Q}^{l\to l} \\ (\boldsymbol{Q}^{l\to l})^H \bar{\boldsymbol{h}}_{SE}^l & \boldsymbol{Q}^{l\to l} + P^{l\to l}\epsilon_l^{-2}\boldsymbol{I}_M \end{bmatrix} \succeq 0. \tag{9}$$

The definition of $\tilde{\boldsymbol{Q}}^{l\to l}$ and $\boldsymbol{Q}^{l\to l}$ are shown in the following section and $P^{l\to l} \geq 0$.

IV. BCD Based Optimization Algorithm Under Imperfect CSI

A. Overall Optimization Framework

In this section, we focus on solving the proposed optimization problem (8). The coupling of different variables and the complicated form of R_S make problem (8) intractable. To cope with this difficulty, we propose the BCD based iterative algorithm to maximize R_S by the beamforming vector optimization of Alice with the fixed passive beamforming of STAR-RIS, followed by the transmission and reflection coefficients optimization with the fixed active beamforming. The details are described next.

In the sequel, the operator $[\cdot]^+$ can be ignored without loss of optimality with a proper selection of C_B and C_E to avoid a negative secrecy rate.

B. Active Beamfomring Optimization

With respect to an active beamforming vector, $\boldsymbol{\omega}_l$, and under fixed passive beamforming $\boldsymbol{\Phi}_l^m$ in the m_{th} iteration of the BCD framework, (8) can be simplified to

$$\max_{\boldsymbol{\omega}_l,\ \tau^{l\to l},\ P^{l\to l}\geq 0, \forall l} \sum_l R_B^{l\to l} - \log_2(1+\tau^{l\to l}) \tag{10a}$$
$$\text{s.t. } (7\text{b}) - (7\text{c}), (7\text{g}), (8\text{c}), (9).$$

Assume that $\boldsymbol{W}_l = \boldsymbol{\omega}_l(\boldsymbol{\omega}_l)^H$, which satisfies $\mathrm{rank}(\boldsymbol{W}_l) = 1$ and $\boldsymbol{W}_l \succeq 0$. Then, we have

$$\left|(\boldsymbol{h}_{SB}^l)^H \boldsymbol{\Phi}_l^m \boldsymbol{h}_{AS}\boldsymbol{\omega}_{l'}\right|^2 = \mathrm{Tr}(\boldsymbol{W}_{l'}(\boldsymbol{H}_{ASB}^l)^H \boldsymbol{H}_{ASB}^l), \quad \forall l, l', \tag{11}$$

where $\boldsymbol{H}_{ASB}^l = (\boldsymbol{h}_{SB}^l)^H \boldsymbol{\Phi}_l^m \boldsymbol{h}_{AS}$. And constraint (7b) can be expressed as

$$\sum_l \mathrm{Tr}(\boldsymbol{W}_l) \leq P_{\max}, \quad \forall l. \tag{12}$$

Further, using $\tilde{\boldsymbol{Q}}^{l\to l} = \tilde{\boldsymbol{Q}}_\omega^{l\to l} = (\bar{\boldsymbol{h}}_{SE}^l)^H \boldsymbol{Q}_\omega^{l\to l} \bar{\boldsymbol{h}}_{SE}^l$ and $\boldsymbol{Q}^{l\to l} = \boldsymbol{Q}_\omega^{l\to l} = -\boldsymbol{\Phi}_l^m \boldsymbol{h}_{AS}\boldsymbol{W}_l(\boldsymbol{\Phi}_l^m \boldsymbol{h}_{AS})^H$, we have the following optimization problem

$$\max_{\boldsymbol{W}_l,\ \tau^{l\to l} P^{l\to l}\geq 0,\ \tilde{R}_B^{l'\to l}, \forall l, l'} \sum_l \tilde{R}_B^{l\to l} - \log_2(1+\tau^{l\to l}) \tag{13a}$$
$$\text{s.t. } \tilde{R}_B^{l'\to l} \leq \log_2(1+\mathrm{SINR}_B^{l'\to l}), \quad \forall l, l', \tag{13b}$$
$$\tilde{R}_B^{l\to l} \geq C_B, \quad \forall l, \tag{13c}$$
$$\boldsymbol{W}_l \succeq 0, \quad \forall l, \tag{13d}$$
$$\mathrm{Rank}(\boldsymbol{W}_l) = 1, \quad \forall l, \tag{13e}$$
$$\tilde{R}_B^{k\to l} \geq \log_2(1+\mathrm{SINR}_B^{l\to l}), \tag{13f}$$
$$\forall \Omega(k) < \Omega(l) (8\text{c}), (9), (12),$$

where $\tilde{R}_B^{l'\to l}$ is the slack variable. Unfortunately, problem (13) is non-convex due to the objective function (13a) and various non-convex constraints, hence, it is solved with the SCA technique. Specifically, since $\log_2(1+\tau^{l\to l})$ is a concave function, with the property that the first order Taylor expansion of a concave function is its over-estimator with the given point $(\tau^{l\to l})^n$ in the n_{th} iteration, we have

$$\begin{aligned}\log_2(1+\tau^{l\to l}) &\leq \log_2(1+(\tau^{l\to l})^n) \\ &\quad + \frac{\log_2 e(\tau^{l\to l} - (\tau^{l\to l})^n)}{1+(\tau^{l\to l})^n} \\ &= (R_E^{l\to l})^{UB}.\end{aligned} \tag{14}$$

Similarly, (13b) and (13f) can be transformed to

$$\begin{aligned}\tilde{R}_B^{l'\to l} \leq\ & \log_2(g_1(\boldsymbol{W}_{l'}) + g_2(\boldsymbol{W}_i, l') + g_3(\boldsymbol{W}_j, l') + \sigma^2) \\ & - \log_2(g_2(\boldsymbol{W}_i^n, l') + g_3(\boldsymbol{W}_j^n, l') + \sigma^2) \\ & - \frac{\log_2 e(\Delta g_2(i, l') + \Delta g_3(j, l'))}{g_2(\boldsymbol{W}_i^n, l') + g_3(\boldsymbol{W}_j^n, l') + \sigma^2},\end{aligned} \tag{15}$$

$$\begin{aligned}\tilde{R}_B^{k\to l} \geq\ & -\log_2(g_2(\boldsymbol{W}_i, k) + g_3(\boldsymbol{W}_j, k) + \sigma^2) \\ & + \log_2(g_1(\boldsymbol{W}_k^n) + g_2(\boldsymbol{W}_i^n, k) + g_3(\boldsymbol{W}_j^n, k) + \sigma^2) \\ & + \frac{\log_2 e(\Delta g_1(k) + \Delta g_2(i, k) + \Delta g_3(j, k))}{g_1(\boldsymbol{W}_k^n) + g_2(\boldsymbol{W}_i^n, k) + g_3(\boldsymbol{W}_j^n, k) + \sigma^2},\end{aligned} \tag{16}$$

where $g_1(\boldsymbol{W}_{l'}) = \mathrm{Tr}(\boldsymbol{W}_{l'}\tilde{\boldsymbol{H}}_{ASB}^l)$, $g_2(\boldsymbol{W}_i, l') = \sum_{\Omega(i)>\Omega(l')} \mathrm{Tr}(\boldsymbol{W}_i\tilde{\boldsymbol{H}}_{ASB}^l)$, $g_3(\boldsymbol{W}_j, l') = \eta \sum_{\Omega(j)<\Omega(l')} \mathrm{Tr}(\boldsymbol{W}_j\tilde{\boldsymbol{H}}_{ASB}^l)$, $\Delta g_1(l') = g_1(\boldsymbol{W}_{l'}) - g_1(\boldsymbol{W}_{l'}^n)$, $\Delta g_2(i, l') = g_2(\boldsymbol{W}_i, l') - g_2(\boldsymbol{W}_i^n, l')$, $\Delta g_3(j, l') = g_3(\boldsymbol{W}_j, l') - g_3(\boldsymbol{W}_j^n, l')$ and $\tilde{\boldsymbol{H}}_{ASB}^l = (\boldsymbol{H}_{ASB}^l)^H \boldsymbol{H}_{ASB}^l$.

Moreover, the condition of equivalence for the rank-one constraint is $\|\boldsymbol{W}_l\|_* - \|\boldsymbol{W}_l\|_2 \leq 0$. With the first order Taylor expansion, the lower bound of $\|\boldsymbol{W}_l\|_2$ is

$$\begin{aligned}\|\boldsymbol{W}_l\|_2 &\geq \|\boldsymbol{W}_l^n\|_2 \\ &\quad + \mathrm{Tr}(\boldsymbol{\mu}_{\max}(\boldsymbol{W}_l^n)\boldsymbol{\mu}_{\max}(\boldsymbol{W}_l^n)^H(\boldsymbol{W}_l - \boldsymbol{W}_l^n)) \\ &= (\|\boldsymbol{W}_l\|_2)^{LB}, \end{aligned} \tag{17}$$

where $\boldsymbol{\mu}_{\max}(\cdot)$ is the eigenvector corresponding to the maximum eigenvalue. We utilize a penalty-based method to replace rank-one constraint with factor $\rho > 0$. Finally, with the given points $(\tau_\omega^{l\to l})^n$, $\boldsymbol{W}_l^n$ and $\boldsymbol{\Phi}_l^m$, the sub-problem of active beamforming can be solved via SCA and is expressed as

$$\max_{\boldsymbol{W}_l, \tau^{l\to l} P^{l\to l} \geq 0, \tilde{R}_B^{l'\to l}, \forall l, l'} \sum_l \tilde{R}_B^{l\to l} - (R_E^{l\to l})^{UB} + \rho((\|\boldsymbol{W}_l\|_2)^{LB} - \|\boldsymbol{W}_l\|_*) \tag{18a}$$

$$\text{s.t. } (8c), (9), (12), (13c) - (13d), (15) - (16).$$

We note that (18) is a convex problem, which can be solved by the CVX tool.

C. Passive Beamforming Optimization

In this section, the passive beamforming of STAR-RIS, e.g. the transmission and reflection coefficients, are optimized. Assume that $\boldsymbol{v}^l = \left[\sqrt{a_1^l}e^{j\phi_1^l}, \sqrt{a_2^l}e^{j\phi_2^l}, \ldots, \sqrt{a_M^l}e^{j\phi_M^l}\right]^H$ and $\boldsymbol{V}_l = \boldsymbol{v}^l(\boldsymbol{v}^l)^H$, which satisfies $\mathrm{rank}(\boldsymbol{V}_l) = 1$ and $\boldsymbol{V}_l \succeq 0$. And STAR-RIS coefficients optimization has a similar structure as the active beamforming optimization. Specifically, we have the following sub-problem for passive beamforming with the given points of $\boldsymbol{\omega}_l^m$, $(\tau^{l\to l})^m$ and $(P^{l\to l})^m$

$$\max_{\boldsymbol{V}_l, \tilde{R}_B^{l'\to l}, \forall l, l'} \sum_l \tilde{R}_B^{l\to l} - \log_2(1 + (\tau^{l\to l})^m) \tag{19a}$$

$$\text{s.t. } \boldsymbol{V}_l \succeq 0, \quad \forall l, \tag{19b}$$

$$\mathrm{Rank}(\boldsymbol{V}_l) = 1, \quad \forall l, \tag{19c}$$

$$\mathrm{diag}\left\{\sum_l \boldsymbol{V}_l\right\} = 1, \quad \forall l, \tag{19d}$$

$$(9), (13b) - (13c), (13f),$$

where $\tilde{R}_B^{l'\to l}$ is the slack variable, and the coefficients of (9) are $\tilde{\boldsymbol{Q}}^{l\to l} = \tilde{\boldsymbol{Q}}_v^{l\to l} = (\bar{\boldsymbol{h}}_{SE}^l)^H \boldsymbol{Q}_v^{l\to l} \bar{\boldsymbol{h}}_{SE}^l$ and $\boldsymbol{Q}^{l\to l} = \boldsymbol{Q}_v^{l\to l} = -\mathrm{diag}\{\boldsymbol{h}_{AS}\boldsymbol{\omega}_l\}\boldsymbol{V}_l(\mathrm{diag}\{\boldsymbol{h}_{AS}\boldsymbol{\omega}_l\})^H$. Next, we handle the non-convex constraints (13b) and (13f) with respect to $\boldsymbol{V}_l$ by SCA. With the first order Taylor expansion, the above constraints can be expressed as

$$\begin{aligned}\tilde{R}_B^{l'\to l} &\leq \log_2(h_1(\boldsymbol{V}_l, l') + h_2(\boldsymbol{V}_l, l') + h_3(\boldsymbol{V}_l, l') + \sigma^2) \\ &\quad - \log_2(h_2(\boldsymbol{V}_l^n, l') + h_3(\boldsymbol{V}_l^n, l') + \sigma^2) \\ &\quad - \frac{\log_2 e(\Delta h_2(l') + \Delta h_3(l'))}{h_2(\boldsymbol{V}_l^n, l') + h_3(\boldsymbol{V}_l^n, l') + \sigma^2}, \end{aligned} \tag{20}$$

$$\begin{aligned}\tilde{R}_B^{k\to l} &\geq -\log_2(h_2(\boldsymbol{V}_l, k) + h_3(\boldsymbol{V}_l, k) + \sigma^2) \\ &\quad + \log_2(h_1(\boldsymbol{V}_l^n, k) + h_2(\boldsymbol{V}_l^n, k) + h_3(\boldsymbol{V}_l^n, k) + \sigma^2) \\ &\quad + \frac{\log_2 e(\Delta h_1(k) + \Delta h_2(k) + \Delta h_3(k))}{h_1(\boldsymbol{V}_l^n, k) + h_2(\boldsymbol{V}_i^n, k) + h_3(\boldsymbol{V}_j^n, k) + \sigma^2}, \end{aligned} \tag{21}$$

Algorithm 1 Overall BCD Based Iterative Algorithm

Initialize: $(\tau_{l\to l})^0$, $\boldsymbol{V}_l^0$, $\boldsymbol{W}_l^0$ and set iteration index $m = 0$.

Repeat

1) Solve (18) with the given points $(\tau_{l\to l})^n$, $\boldsymbol{W}_l^n$, and $\boldsymbol{V}_l^m$ under the SCA scheme.
2) Solve (22) with the given points $\boldsymbol{V}_l^n$, $(\tau_{l\to l})^m$, and $\boldsymbol{W}_l^m$ under the SCA scheme, and set $m = m + 1$.

Until $R_S^{(m)} - R_S^{(m-1)} \leq \epsilon_R$ or $m > m_{\max}$.

where $h_1(\boldsymbol{V}_l, l') = \mathrm{Tr}(\boldsymbol{V}_l(\boldsymbol{G}_{ASB}^l)^H \boldsymbol{W}_{l'}^m \boldsymbol{G}_{ASB}^l)$, $h_2(\boldsymbol{V}_l, l') = \sum_{\Omega(i) > \Omega(l')} \mathrm{Tr}(\boldsymbol{V}_l(\boldsymbol{G}_{ASB}^l)^H \boldsymbol{W}_i^m \boldsymbol{G}_{ASB}^l)$, $h_3(\boldsymbol{V}_l, l') = \eta \sum_{\Omega(j) < \Omega(l')} \mathrm{Tr}(\boldsymbol{V}_l(\boldsymbol{G}_{ASB}^l)^H \boldsymbol{W}_j^m \boldsymbol{G}_{ASB}^l)$, $\Delta h_1(l') = h_1(\boldsymbol{V}_l, l') - h_1(\boldsymbol{V}_l^n, l')$, $\Delta h_2(l') = h_2(\boldsymbol{V}_l, l') - h_2(\boldsymbol{V}_l^n, l')$, $\Delta h_3(l') = h_3(\boldsymbol{V}_l, l') - h_3(\boldsymbol{V}_l^n, l')$ and $\boldsymbol{G}_{ASB}^l = (\mathrm{diag}\left\{(\boldsymbol{h}_{SB}^l)^H\right\} \boldsymbol{h}_{AS})^H$. The rank-one constraint of $\boldsymbol{V}_l$ is relaxed with the same operation of $\boldsymbol{W}_l$ by the subtraction of the nuclear norm and the spectral norm. Hence, with the given points $\boldsymbol{\omega}_l^m$, $(\tau^{l\to l})^m$, $(P^{l\to l})^m$, and $\boldsymbol{V}_l^n$, the passive beamforming optimization can be expressed as

$$\max_{\boldsymbol{V}_l, \tilde{R}_B^{l'\to l}, \forall l, l'} \sum_l \tilde{R}_B^{l\to l} - \log_2(1 + (\tau^{l\to l})^m) + \rho((\|\boldsymbol{V}_l\|_2)^{LB} - \|\boldsymbol{V}_l\|_*) \tag{22a}$$

$$\text{s.t. } (9), (13c), (19b), (19d), (20) - (21),$$

where the definition of $(\|\boldsymbol{V}_l\|_2)^{LB}$ is similar to $(\|\boldsymbol{W}_l\|_2)^{LB}$. Therefore, the passive beamforming optimization is transformed to the convex problem (22), which can be solved effectively by the CVX tool.

D. Complexity and Convergence Analysis

Herein, the BCD based optimization algorithm under imperfect CSI is proposed to maximize the worst secrecy rate. The overall algorithm is shown in **Algorithm 1**. Furthermore, the complexity of **Algorithm 1** is $\mathcal{O}(N_3(N_1\sqrt{K+1}(3(K+1)^3 + 9(K+1)^2 + 27)) + N_2\sqrt{M+1}(4(M+1)^3 + 16(M+1)^2 + 64)))$ [17], where N_1, N_2, and N_3 are the number of iterations for the active beamforming optimization inner loop, the passive beamforming optimization inner loop, and the overall BCD based algorithm. Furthermore, problems (18) and (22) give the lower bound of (7), which illustrates that the objective function is non-decreasing and **Algorithm 1** is guaranteed to converge.

V. Implementation and Performance Analysis

In this section, numerical results are utilized to illustrate the performance of the proposed algorithm. The coordinates of Alice and STAR-RIS are $(0, -100, 10)$ and $(0, 0, 10)$. Bobs at the reflection range and the transmission range are located at $(-5, -5, 2)$ and $(5, 5, 2)$, and the corresponding Eves are located at $(0, -50, 2)$ and $(0, 50, 2)$ [8]. The channel coefficients are set to $\beta = 5$dB and $\alpha = 2.2$. The normalized estimation error of the Eves $\delta_l = \delta_{l'} = \delta = \epsilon / \left\|\bar{\boldsymbol{h}}_{SE}^l\right\|$ defined in [15] is considered in this letter. There are $M = 12$ elements on STAR-RIS, the maximum transmission power of Alice is $P_{\max} = 30$dBm, the number of antennas is 4 and $\eta = 0.01$ unless specified otherwise. Furthermore, the conventional RIS (C-RIS), STAR-RIS based on TS-OMA and

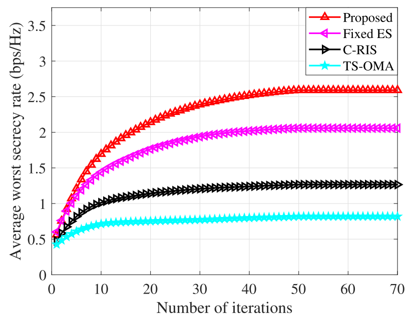

Fig. 2. Convergence of proposed algorithm.

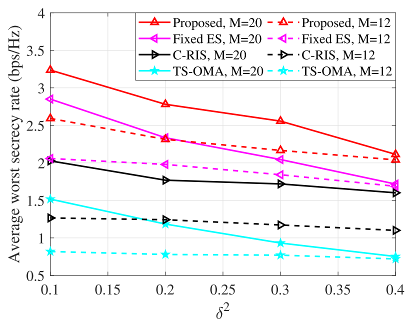

Fig. 3. Average worst secrecy rate versus δ^2.

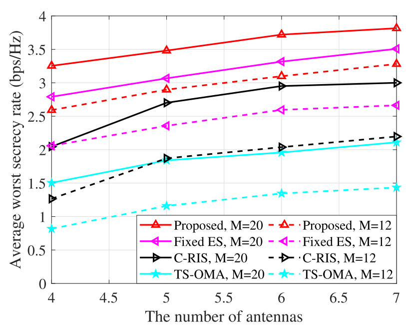

Fig. 4. Average worst secrecy rate versus K.

STAR-RIS with fixed ES protocol under $a_m^r = a_m^t = 0.5$ are also included in the simulation. In particular, C-RIS can be regarded as a reflection only RIS and a transmission only RIS under the adjacent deployment with $M/2$ elements, whose coefficients can be obtained by **Algorithm 1** with power constraint $a_m^l = 1, \forall l, m$. The coefficients of STAR-RIS with TS-OMA can also be obtained by **Algorithm 1** under some simple modifications, that replace (19d) with $\mathrm{diag}\{\boldsymbol{V}_l\} = 1$.

As illustrated in Fig. 2, **Algorithm 1** converges in the limit iterations for all the schemes in the case of $M = 12$ and $K = 4$, where the compatibility of our proposed algorithm with TS-OMA and C-RIS is proved. In Fig. 3, our proposed algorithm achieves higher R_S for different δ^2 compared with other schemes under $M = 20$ (solid line) and $M = 12$ (dotted line), which explains that the independent adjustment of reflection and transmission elements of STAR-RIS is more efficient than C-RIS for secure NOMA systems. And the restricted SE of TS-OMA makes it not sufficient enough for secure NOMA communications. Further, the performance of dynamic ES allocation exceeds that of the fixed ES protocol, which illustrates that $a_m^r + a_m^t = 1$ is a better option than $a_m^r = a_m^t = 0.5$.

Furthermore, from Fig. 4, it is observed that R_s is increasing with the number of antennas at Alice due to the stronger active beamforming gain for all the schemes. Compared with other techniques, our proposed algorithm achieves superior average worst secrecy rate with the different number of antennas. With respect to engineering insights, the required hardware cost such as the number of STAR-RIS elements and antennas on BS is fewer than C-RIS for a given secrecy rate, which improves the flexibility of deployment significantly.

VI. Conclusion

In this letter, we model the STAR-RIS enabled downlink secure MISO NOMA network under the ES protocol with imperfect CSI, and propose the BCD based optimization algorithm by SCA and a penalty-based method with respect to active beamforming at Alice and STAR-RIS coefficients, where the uncertainty of Eve's CSI is handled by *S-Procedure*. Simulation results show that our proposed algorithm has greater average worst secrecy rate compared with C-RIS, TS-OMA, and fixed ES protocol under various simulation settings, which proves that the independent optimization for the amplitude and phase of STAR-RIS is effective, and the superior SE of the ES protocol for NOMA improves the security compared with the TS-OMA scheme.

References

[1] Q. Wu and R. Zhang, "Towards smart and reconfigurable environment: Intelligent reflecting surface aided wireless network," *IEEE Commun. Mag.*, vol. 58, no. 1, pp. 106–112, Nov. 2020.
[2] Y. Liu et al., "STAR: Simultaneous transmission and reflection for 360° coverage by intelligent surfaces," *IEEE Wireless Commun.*, vol. 28, no. 6, pp. 102–109, Dec. 2021.
[3] G. Gui et al., "6G: Opening new horizons for integration of comfort, security, and intelligence," *IEEE Wireless Commun.*, vol. 27, no. 5, pp. 126–132, Oct. 2020.
[4] C. Wu et al., "Coverage characterization of STAR-RIS networks: NOMA and OMA," *IEEE Commun. Lett.*, vol. 25, no. 9, pp. 3036–3040, Sep. 2021.
[5] X. Mu et al., "Simultaneously transmitting and reflecting (STAR) RIS aided wireless communications," *IEEE Trans. Wireless Commun.*, vol. 21, no. 5, pp. 3083–3098, May 2022.
[6] Y. Wang et al., "Transmit power optimization of simultaneous transmission and reflection RIS assisted full-duplex communications," *IEEE Access*, vol. 10, pp. 61192–61200, 2022.
[7] H. Niu et al., "Simultaneous transmission and reflection reconfigurable intelligent surface assisted secrecy MISO networks," *IEEE Commun. Lett.*, vol. 25, no. 11, pp. 3498–3502, Nov. 2021.
[8] Y. Han et al., "Artificial noise aided secure NOMA communications in STAR-RIS networks," *IEEE Wireless Commun. Lett.*, vol. 11, no. 6, pp. 1191–1195, Jun. 2022.
[9] Z. Zhang et al., "On the secrecy design of STAR-RIS assisted uplink NOMA networks," *IEEE Trans. Wireless Commun.*, vol. 21, no. 12, pp. 11207–11221, Dec. 2022.
[10] L. Lv et al., "Covert communication in intelligent reflecting surface-assisted NOMA systems: Design, analysis, and optimization," *IEEE Trans. Wireless Commun.*, vol. 21, no. 3, pp. 1735–1750, Mar. 2022.
[11] S. Hu et al., "Robust and secure sum-rate maximization for multiuser MISO downlink systems with self-sustainable IRS," *IEEE Trans. Commun.*, vol. 69, no. 10, pp. 7032–7049, Oct. 2021.
[12] X. Yu et al., "Smart and reconfigurable wireless communications: From IRS modeling to algorithm design," *IEEE Wireless Commun.*, vol. 28, no. 6, pp. 118–125, Dec. 2021.
[13] C. Zhang et al., "STAR-IOS aided NOMA networks: Channel model approximation and performance analysis," *IEEE Trans. Wireless Commun.*, vol. 21, no. 9, pp. 6861–6876, Sep. 2022.
[14] X. Guan et al., "Anchor-assisted channel estimation for intelligent reflecting surface aided multiuser communication," *IEEE Trans. Wireless Commun.*, vol. 21, no. 6, pp. 3764–3778, Jun. 2022.
[15] X. Yu et al., "Robust and secure wireless communications via intelligent reflecting surfaces," *IEEE J. Sel. Areas Commun.*, vol. 38, no. 11, pp. 2637–2652, Nov. 2020.
[16] Z.-Q. Luo et al., "Multivariate nonnegative quadratic mappings," *SIAM J. Optim.*, vol. 14, no. 4, pp. 1140–1162, Jul. 2004.
[17] I. Pólik et al., *Interior Point Methods for Nonlinear Optimization*. Berlin, Germany: Springer, 2010.